Dielectric relaxation and conductivity behavior in modified lead titanate ferroelectric ceramics

2008 J. Phys.: Condens. Matter 20 505208

(http://iopscience.iop.org/0953-8984/20/50/505208)

J. Phys.: Condens. Matter **20** (2008) 505208 (10pp) doi:10.1088/0953-8984/20/50/505208

Dielectric relaxation and conductivity behavior in modified lead titanate ferroelectric ceramics

A Peláiz-Barranco[1,3], Y González Abreu[1] and R López-Noda[2]

[1] Facultad de Física-Instituto de Ciencia y Tecnología de Materiales, Universidad de La Habana. San Lázaro y L, Vedado. La Habana 10400, Cuba
[2] Departamento de Física Aplicada, Instituto de Cibernética, Matemática y Física, ICIMAF, CITMA 15 # 551, Vedado. La Habana 10400, Cuba

E-mail: pelaiz@fisica.uh.cu

Received 3 August 2008, in final form 15 October 2008
Published 12 November 2008
Online at stacks.iop.org/JPhysCM/20/505208

Abstract
The frequency and temperature dielectric response and the electrical conductivity behavior around the ferroelectric–paraelectric phase transition temperature are studied in the ferroelectric ceramic system $(Pb_{0.88}Sm_{0.08})(Ti_{1-x}Mn_x)O_3$, with $x = 0$, 1, 3 at.%. The contribution of the conductive processes to the dielectric relaxation for the studied frequency range is discussed considering the oxygen vacancies as the most mobile ionic defects in perovskites, whose concentration seems to increase with the manganese content. The relaxation processes below the transition temperature are associated with the decay of the polarization in the oxygen-defect-related dipoles due to their hopping conduction. Above the ferroelectric–paraelectric phase transition temperature, the electrical conduction is governed by the thermal excitation of carriers from oxygen vacancies; the relaxation processes are associated with ionic dipoles distorted by the oxygen vacancies.

1. Introduction

Lead titanate ($PbTiO_3$) is one of the potential useful ferroelectric materials with a highly polar perovskite structure (ABO_3) [1–3], showing a high electromechanical anisotropy in the piezoelectric effect. It is well known that $PbTiO_3$ (PT) undergoes a single ferroelectric transition from cubic to tetragonal [1] at around 490 °C, whereby the polar tetragonal state is stabilized by the large tetragonal strain in the *c* axis brought about by Pb–O hybridization. Systematic studies of the crystal structures, microstructures and electrical properties on modified PT have been developed in the last decades [1–12]. The sintering of pure PT ceramics is very difficult because of the large tetragonality, which it has been shown can be reduced greatly by the partial substitution of the Pb^{2+} or Ti^{4+} ions [1–6, 9–12]. It is known that dense ceramics could be obtained by the partial substitution of rare earth elements in modified lead titanate [9, 10, 13–16], which conserves the electromechanical anisotropy in the piezoelectric effect. The inherent anisotropy in the piezoelectric effect depends on the degree of microstress and structural defects, including the random distribution of oxygen defects, which are present in these materials. These results make these ceramics suitable for high-frequency devices since the spurious wave generation in the acoustic signal is very small for lateral vibration, in contrast with traditional transducers based on the lead zirconate titanate (PZT) ceramic system [17].

The introduction of rare earth (Ln^{3+}) into lead titanate produces one lead vacancy for every two Ln^{3+} ions. These defects locally break the translational periodicity of the lattice and then the long-range interaction between ferroelectrically active octahedra containing B-site cations is affected. On the other hand, a modification on the B site provides an optimum electromechanical anisotropy. It has been shown that modification by using manganese, which occupies B sites, provides new structural defects, i.e. oxygen vacancies, produced by Mn^{4+}/Mn^{2+} reduction, during the sintering process [10, 18, 19].

Although many studies have been developed on the $(Pb, Ln)(Ti, Mn)O_3$ system [9, 10, 13–16, 18, 19], the effects of manganese reduction during sintering have not been usually

[3] Author to whom any correspondence should be addressed.

considered, which should play an important role in the piezoelectric behavior because of the introduction of oxygen vacancies to compensate for the charge imbalance. The oxygen vacancy concentration in rare earth and manganese modified lead titanate could have an important contribution to the electrical response of these materials, i.e. the dielectric relaxation processes and also the electrical conductivity behavior.

The present paper describes a study on the dielectric relaxation and the electrical conductivity behavior of modified lead titanate ferroelectric ceramics $(Pb_{0.88}Sm_{0.08})(Ti_{1-x}Mn_x)O_3$, $x = 0$, 1, 3 at.%, named PSTM-x, in a wide frequency range around the ferroelectric–paraelectric phase transition temperature. The frequency and temperature behavior of the complex dielectric permittivity are analyzed considering the semi-empirical complex Cole–Cole equation, the universal relaxation law and the Dissado–Hill theory.

2. Experimental procedure

$(Pb_{0.88}Sm_{0.08})(Ti_{1-x}Mn_x)O_3$, $x = 0$, 1, 3 at.%, ceramic powders were prepared via the mixed-oxide route [1]. The starting powders were mixed and calcined at 900 °C for 2 h in air. Sintering was then performed at 1200 °C for two additional hours in air in a well covered platinum crucible in order to minimize the evaporation of reagents. X-ray diffraction analysis at room temperature was performed on powder samples by using a Rigaku Rotaflex RU200B diffractometer (Rigaku Corporation, Tokyo Branch, Japan) and Cu Kα radiation. Silver painted electrodes were applied to the opposite faces of sintered samples by a heat treatment at 590 °C. Capacitance and dielectric losses were measured by a QuadTech 1750 *LCR* bridge (QuadTech, Inc., USA), over the frequency range of 20 Hz–200 kHz. The measurements were performed from room temperature up to 500 °C approximately, applying 1 V ac to the samples. The real and imaginary parts of the dielectric permittivity were obtained with the appropriated geometrical factor. The conductivity data ($\sigma(\omega)$) were obtained with the appropriated geometric factor by using equation (1),

$$\sigma(\omega) = \varepsilon_0 \omega \varepsilon''(\omega) \tag{1}$$

where ε_0 is the vacuum dielectric permittivity, ω is the angular frequency and $\varepsilon''(\omega)$ is the frequency dependence of the imaginary part of the dielectric permittivity.

3. Results and discussion

X-ray diffraction spectra of the $(Pb_{0.88}Sm_{0.08})(Ti_{1-x}Mn_x)O_3$ (PSTM-x) ceramics are shown in figure 1. The indexation is the same for all compositions. A tetragonal perovskite phase was obtained for the studied samples. Table 1 shows the lattice parameters, where it can be seen that there is no significant effect of the manganese on the structural parameters. This result agrees with other reports for similar materials [19]. The ionic radius of the Mn^{2+} ion is similar to that of the Ti^{4+} ion (0.81 and 0.74 Å, respectively, considering the corresponding coordination number for the B site of

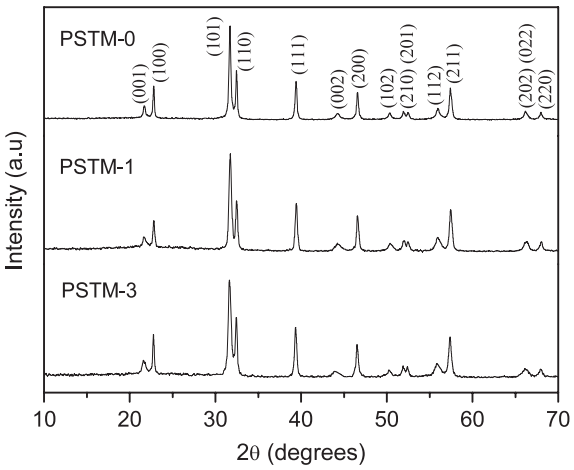

Figure 1. X-ray diffraction patterns of the studied samples at room temperature.

Table 1. Lattice parameters for the studied compositions at room temperature.

	a (Å)	c (Å)	c/a
PSTM-0	3.896	4.088	1.050
PSTM-1	3.896	4.085	1.048
PSTM-3	3.899	4.090	1.049

the perovskite structure) [20] and thereby upon manganese substitution an important effect on the structural parameters is not expected. Note that we have considered Mn^{2+} because previous studies have shown that a Mn^{4+}/Mn^{2+} reduction takes place during the sintering process for this type of materials [10, 18, 19].

Results obtained for the dielectric response of the studied ceramics are shown in figure 2. There is shown the temperature dependence of the real (ε') and imaginary (ε'') parts of the dielectric permittivity for three frequencies, as an example of the investigated behavior for the whole frequency range. Two peaks or inflections associated with these were observed in the temperature dependence of the real part of the dielectric permittivity for the studied frequency range. The first one was observed at 340 °C for the studied samples. The second one was observed for PSTM-1 and PSTM-3 around 425 °C and for PSTM-0 above 450 °C, respectively. The temperature corresponding to the first peak (lower temperature, i.e. at 340 °C) is associated with the ferroelectric–paraelectric phase transition (T_m) considering previous reports for these materials [21, 22]. The manganese ion incorporation in the B site of the perovskite structure does not show a significant effect on T_m. These results agree with previous reports for similar materials [19, 23]. The ferroelectricity results from a condensing of a transverse optical phonon mode at the center of the Brillouin zone, which results from long-range Coulomb interactions between atomic dipole moments. For PT type materials, the stability of the long-range interactions is believed to be suppressed by decoupling effects caused by the incorporation of ions on the A site of the perovskite structure. Therefore, the samarium modified PT ceramics show lower

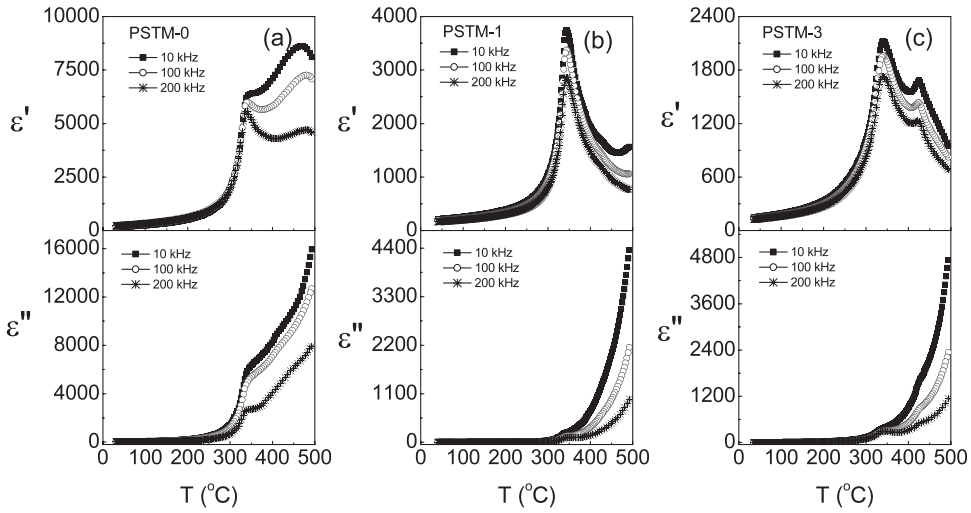

Figure 2. Temperature dependence of the real (ε') and imaginary (ε'') parts of the dielectric permittivity for (a) PSTM-0, (b) PSTM-1, and (c) PSTM-3. The results are shown for three frequencies, as an example of the observed behavior in the studied frequency range.

T_m values than that of the non-modified lead titanate (T_m = 490 °C). However, the manganese ions substitute for Ti^{4+} ions in the B sites of the perovskite structure. Therefore, upon manganese substitution an important effect on phase transition temperature T_m is not expected.

For all the cases, the temperature associated with the ferroelectric–paraelectric phase transition temperature (T_m) did not show any frequency dependence, which is typical of 'normal' ferroelectric–paraelectric- phase transitions. On the other hand, the loss factor (ε'') showed a peak at the same temperature as that observed for the real part of the dielectric permittivity (T_m). The 'normal' characteristic of the phase transition was confirmed by the temperature dependence of ε'' as a function of the frequency where no frequency dispersion of the temperature of maximum dielectric permittivity was observed. A sudden increase of ε'' was obtained for temperatures around 400 °C for all the studied compositions. This behavior could be associated with high conductivity values, which promotes the increase of the dielectric losses.

The presence of two peaks in the temperature dependence of ε' has been previously observed in $(Pb_{0.88}Ln_{0.08})(Ti_{0.98}Mn_{0.02})O_3$[Ln = La, Nd, Sm, Gd, Dy, Ho, Er] ferroelectric ceramics [24, 25]. For the small-radius ions (Dy, Ho, and Er) a strong increment of the tetragonality was observed [24], even above the pure lead titanate. Both peaks were associated with ferroelectric–paraelectric phase transitions concerning two different contributions to the total dielectric behavior of the samples: one in which the rare earth ions occupy the A sites and another one where the ions occupy the B sites of the perovskite structure [24]. For the large-radius ions (La, Nd, Sm and Gd) the analysis has shown that, even when an eventual incorporation of the rare earth into the A and/or B sites of the perovskite structure could be possible, both peaks could not be associated with ferroelectric–paraelectric phase transitions. The observed peak at the lower temperatures has been associated with the ferroelectric–paraelectric phase transition, whereas the hopping of oxygen vacancies has been considered as the cause for the dielectric anomaly at the higher temperatures [25].

In this paper we are not going to discuss the dielectric behavior of the studied samples concerning the second peak. The objective of this paper is the study of the dielectric relaxation phenomenon and the electrical conductivity below and above the first peak, i.e. below and above the temperature of the ferroelectric–paraelectric phase transition (T_m = 340 °C for all the studied samples).

In ferroelectrics, the dielectric relaxation phenomenon reflects the delay (time dependence) in the frequency response of a group of dipoles subjected to an external applied field. When an alternating current is applied to a sample, the dipoles responsible for the polarization are no longer able to follow the oscillations of the electric field at certain frequencies. The field reversal and the dipole reorientation become out of phase, giving rise to a dissipation of energy. Over a wide frequency range, different types of polarization cause several dispersion regions, and the critical frequency characteristic of each contributing mechanism depends on the nature of the dipoles. For ferroelectric materials the dielectric relaxations are very sensitive to both external (temperature, electric field, ionic substitution, etc) and intrinsic (defect, domain configuration, etc) modifications because the polarization is greatly affected. The defects depend on either intrinsic or extrinsic heterogeneities due to special heat treatments (quenching, annealing, etc), ionic substitutions, grain size additives, and grain boundary nature. Defects may cause modifications of the short- and/or long-range interactions in ferroelectrics.

The main dielectric function generally used to describe the dielectric dispersion is the complex dielectric permittivity. The investigation of the complex dielectric permittivity over a wide frequency range, i.e. the dielectric spectrum, is necessary to study relaxations. The main dielectric function generally used to describe the dielectric relaxation is the complex permittivity. In polar dielectrics, corrections to the simple Debye model are often necessary. Cole–Cole plots reflect the deviation from the

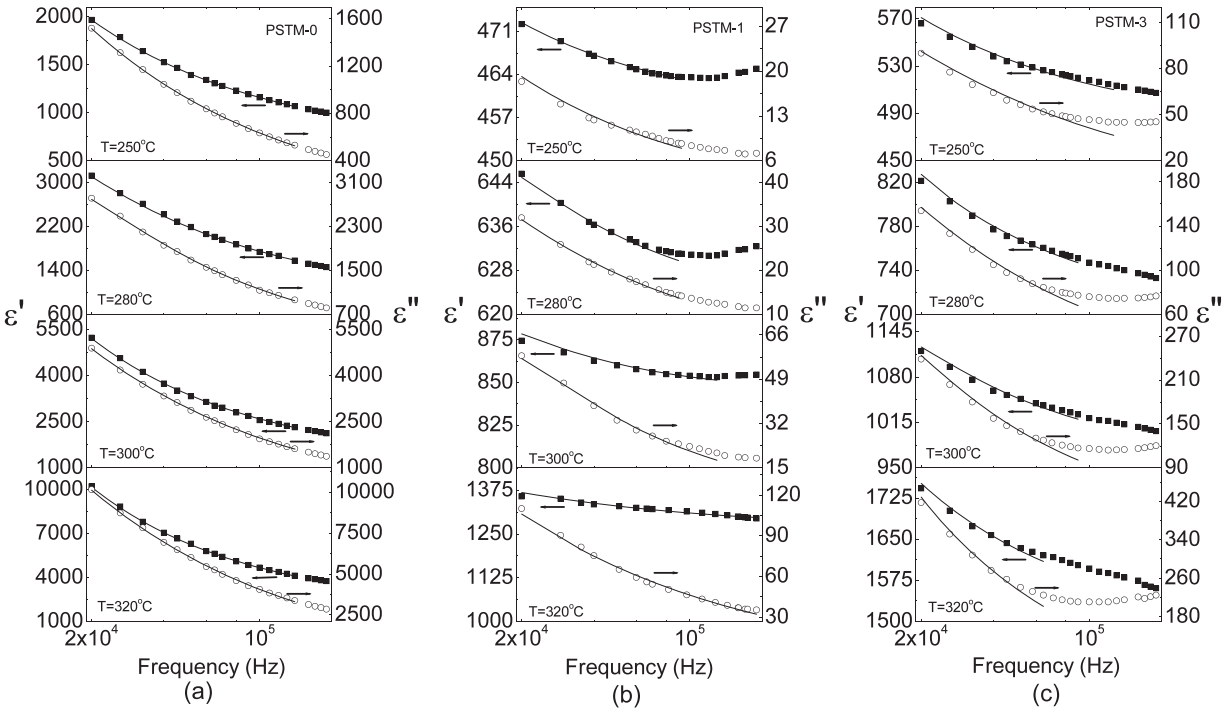

Figure 3. Frequency dependence of the real ε' (■) and imaginary ε'' (○) parts of the dielectric permittivity at a few representative temperatures below T_m for (a) PSTM-0, (b) PSTM-1, and (c) PSTM-3. Solid lines represent the fitting using equations (2) and (3).

ideal Debye model and introduce a parameter which reflects a distribution of the relaxation time. Following the semi-empirical complex Cole–Cole equation [26], the real (ε') and imaginary (ε'') parts of the complex dielectric permittivity can be written as

$$\varepsilon'(\omega) = \varepsilon_\infty + \left(\frac{\Delta\varepsilon'}{2}\right)\left\{1 - \frac{\sinh(\beta z)}{\cosh(\beta z) + \cos\left(\beta\frac{\pi}{2}\right)}\right\} \quad (2)$$

$$\varepsilon''(\omega) = \left(\frac{\Delta\varepsilon'}{2}\right)\frac{\sin\left(\beta\frac{\pi}{2}\right)}{\cosh(\beta z) + \cos\left(\beta\frac{\pi}{2}\right)} \quad (3)$$

where $z = \ln(\omega\tau)$, $\Delta\varepsilon' = \varepsilon_s - \varepsilon_\infty$, ε_∞ is the dielectric permittivity at high frequency, ε_s is the static dielectric permittivity, ω is the angular frequency, τ is the mean relaxation time and $\beta = (1 - \alpha)$, where α shows the deformation of the semi-circle arc in the Cole–Cole plot, i.e., it is the angle from the ε' axis to the center of the semi-circle arc.

3.1. Below T_m ($T < T_m$)

Figure 3 shows the frequency dependence of the real (ε') and imaginary (ε'') parts of the dielectric permittivity at a few representative temperatures below $T_m = 340\,°C$. Solid lines represent the fitting using equations (2) and (3). There is good agreement between theoretical (solid lines) and experimental values (symbols). Note that the fitting is not so good at high frequencies in some of the cases. This has been associated with processes occurring at higher frequencies, which should be studied considering a wide frequency range above 200 kHz. Table 2 shows the corresponding adjusting parameters, β, ε_S, ε_∞, and τ, for the studied samples.

Table 2. Adjusting parameters below T_m, obtained from the fitting using equations (2) and (3).

T (°C)	Composition	β	ε_S	ε_∞	τ (s)
250	PSTM-0	0.6	34 346	632	0.001 030
	PSTM-1	0.6	920	457	0.001 071
	PSTM-3	0.6	1272	479	0.000 149
280	PSTM-0	0.6	36 357	866	0.000 358
	PSTM-1	0.6	1106	619	0.000 420
	PSTM-3	0.6	1972	694	0.000 064
300	PSTM-0	0.6	52 567	1155	0.000 201
	PSTM-1	0.6	1664	841	0.000 224
	PSTM-3	0.6	2736	946	0.000 041
320	PSTM-0	0.6	88 041	1845	0.000 108
	PSTM-1	0.6	2101	1272	0.000 126
	PSTM-3	0.7	3382	1557	0.000 029

The relaxation processes are described by an Arrhenius behavior for the mean relation time, as shown in equation (4),

$$\tau = \tau_0 \exp\left(\frac{E_a}{k_B T}\right) \quad (4)$$

where E_a is the activation energy of the relaxation process, k_B is the Boltzmann's constant, T is the temperature and τ_0 is the pre-exponential factor. Figure 4 shows the Arrhenius behavior corresponding to the mean relaxation time values obtained from the fitting shown in figure 3. The activation energy values (see figure 4) show that the dielectric relaxation processes in the studied samples are closely related to the oxygen vacancies, which have been reported as the most mobile ionic defects in perovskites [27]. According to Steinsvik *et al* [28], the activation energy in the ABO_3

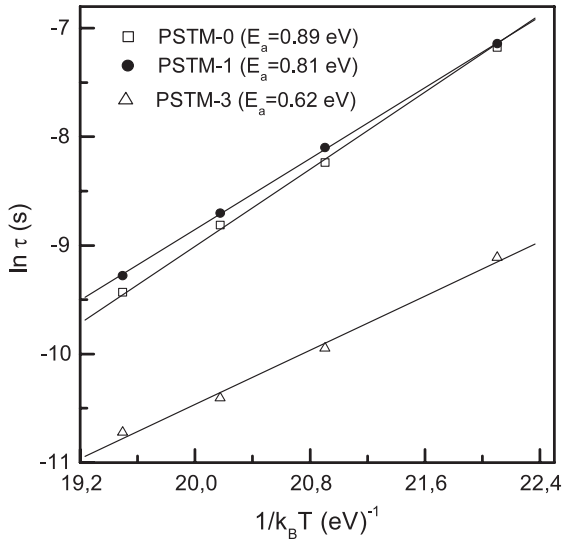

Figure 4. Arrhenius dependence for the relaxation time below T_m for the studied samples, obtained from the fitting shown in figure 3 by using equations (2) and (3).

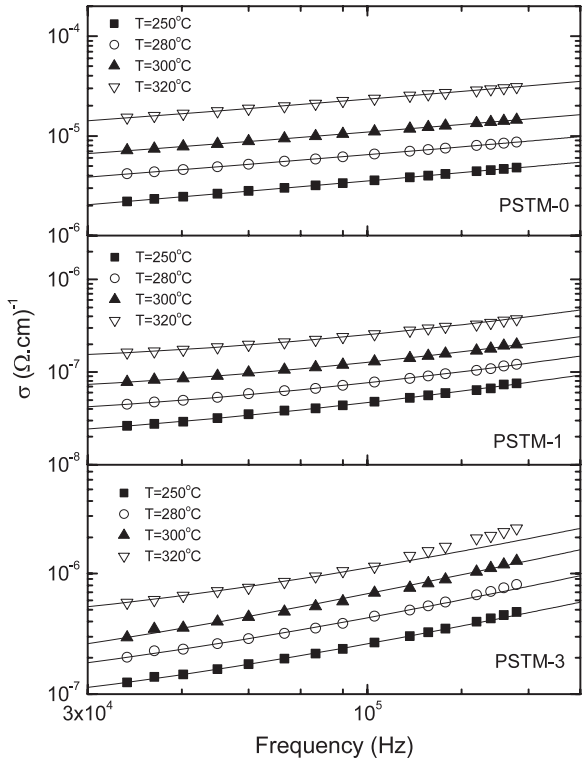

Figure 5. Frequency dependent conductivity data at a few representative temperatures below the ferroelectric–paraelectric phase transition ($T_m = 340\,°C$) for PSTM-0, PSTM-1, and PSTM-3. Solid lines represent the fitting using the UDR term of equation (5) for PSTM-0 and PSTM-1, and both terms (UDR +NCL) for PSTM-3.

perovskite structure decreases with increasing oxygen vacancy content. For the studied samples, the activation energy values decrease with the manganese content, which suggests an increase of oxygen vacancy concentration [28]. Electronic paramagnetic resonance (EPR) studies in rare earth and manganese modified lead titanate ceramics have shown that a Mn^{4+}/Mn^{2+} reduction takes place during the sintering process [18, 19]. As a consequence, oxygen vacancies have to be created to compensate for the charge imbalance. The increase of manganese content should promote a higher concentration of oxygen vacancies, which agrees with the decrease of activation energy values.

For the PT-based ceramic samples [1], the spontaneous polarization originating from the ionic or dipole displacement is known to be the center offset displacement of Ti^{4+} ions from the anionic charge center of the oxygen octahedron. The presence of oxygen vacancies in the studied samples would distort the ionic dipoles due to the Ti^{4+} ions. Thus, the decay of polarization due to distorted ionic dipoles could be the cause for the dielectric relaxation process. However, the previously reported activation energy values [29], which have been associated with relaxations involving thermal motions of Ti^{4+}, are higher than those reported for the studied samples (above 1.2 eV). Due to this, relaxations involving thermal motions of Ti^{4+} are not a probable process. The observed relaxation process for the studied ceramics could be attributed to the decay of polarization in the oxygen-defect-related dipoles due to their hopping conduction.

The frequency dependent conductivity can be described by the known augmented Jonscher relation [30] as

$$\sigma(\omega) = \sigma_{dc}\left[1 + \left(\frac{\omega}{\omega_H}\right)^n\right] + A\omega \qquad (5)$$

where σ_{dc}, ω_H, n, and A are the dc conductivity, the onset frequency of the ac conductivity (mean frequency of the hopping process), the exponent, and the weakly temperature dependent term, respectively. The first and the second terms of equation (5) refer to the universal dielectric response (UDR) and to the nearly constant loss (NCL), respectively.

The power-law frequency dependent term (UDR) originates from the hopping of the carriers with interactions of the inherent defects in the materials, while the origin of the NCL term (the linear frequency dependent term) has been associated with rocking motions in an asymmetric double well potential [31]. For the NCL term, the electrical losses occur during the time regime while the ions are confined to the potential energy minimum [32].

Figure 5 shows the frequency dependent conductivity at a few representative temperatures below T_m for the studied series compositions. The data were analyzed considering the UDR term, the NCL term, and both terms of the Jonscher's relation (equation (5)). Only the UDR term offered a good agreement with the experimental data (solid lines in figure 5) for PSTM-0 and PSTM-1. For PSTM-3, a good fitting was obtained by using both terms of equation (5). For all samples, the n exponent only shows a small temperature dependence, in agreement with previous reports [31].

Both the dc conductivity and the hopping frequency are found to be thermally activated following an Arrhenius dependence (equations (6) and (7)), U_{dc} and U_H being the activation energies of the dc conductivity and the hopping

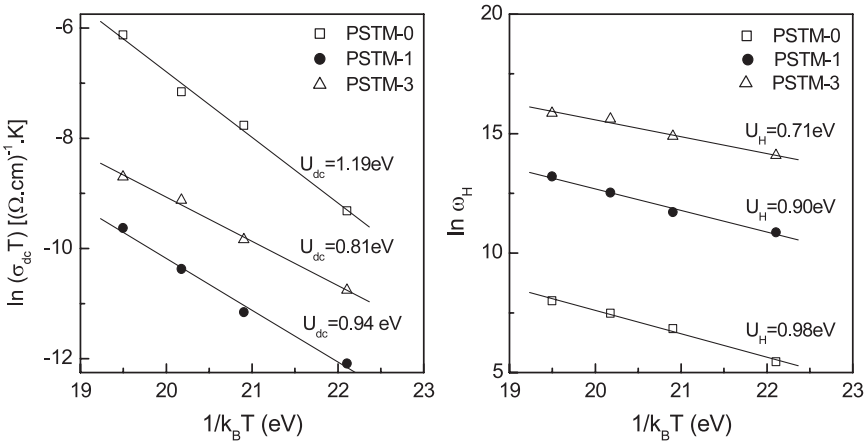

Figure 6. Arrhenius dependence for the dc conductivity (σ_{dc}) and the hopping frequency (ω_H) below T_m for the studied samples. The solid lines are the respective linear fits using equations (6) and (7).

frequencies of the carriers, respectively, and σ_0 and ω_0 the pre-exponential factors. This has been interpreted using different theoretical models [30, 33, 34] as indicating that the ac conductivity originates from a migration of ions by hopping between neighboring potential wells, which eventually gives rise to a dc conductivity at the lowest frequencies.

$$\sigma_{dc}T = \sigma_0 \exp\left(\frac{-U_{dc}}{k_B T}\right) \tag{6}$$

$$\omega_H = \omega_0 \exp\left(\frac{-U_H}{k_B T}\right). \tag{7}$$

Figure 6 shows the Arrhenius dependence for both parameters for the studied samples below T_m, which were obtained from the fitting of the experimental data shown in figure 5. The solid lines represent the fitting using equations (6) and (7). The corresponding activation energy values are shown in the same figure.

The ranges of activation energy values for the dc conductivity are very close to the activation energy values of the ionic conductivity by oxygen vacancies in perovskite type ferroelectric oxides [35–37]. Values in the ranges 0.3–0.4 eV and 0.6–1.2 eV have been associated with singly [38, 39] and doubly ionized [40, 41] oxygen vacancies, respectively, for different perovskite oxides. On the basis of the calculated value of activation energy for the dc conductivity, it can be concluded that oxygen vacancies are the most likely charge carriers operating in these ceramics below T_m. At room temperature, the oxygen vacancies exhibit a low mobility, whereby the ceramic samples exhibit an enhanced resistance. However, with rising temperature, they are activated and contribute to the observed electrical behavior. In addition, the dielectric relaxations occurring at low frequency are related to the space charges in association with these oxygen vacancies, which can be trapped at the grain boundaries or electrode–sample interface.

The presence of oxygen vacancies is expected only for Mn doped (Pb, Sm)TiO_3 due to the Mn^{4+}/Mn^{2+} reduction process that takes place during the sintering process of the samples, as was analyzed by electronic paramagnetic resonance (EPR) [18, 19]. However, oxygen vacancies are easily induced during the sintering process because the PbO lower volatile temperature is about 900 °C. This phenomenon takes place in all samples and also promotes lead vacancies, which are quenched defects at low temperature. The lead vacancies could only become mobile at high temperatures with high activation energy values [42]. The increment in manganese addition promotes a higher concentration of oxygen vacancies, which are the mobile charges, providing a decrement in the U_{dc} activation energy values.

On the other hand, the activation energy values for the hopping processes (U_H) are not very far from the U_{dc} values, showing that the hopping processes could be related to the movement of the oxygen vacancies. The short-range hopping of oxygen vacancies, similar to the reorientation of the dipole, could lead to the relaxation processes. Note that the increment in manganese concentration provides the decrease in U_H too. Considering that the relaxation processes have been associated with the oxygen vacancies, the increment of their concentration should provide the observed behavior.

3.2. Above T_m ($T > T_m$)

Figure 7 shows the frequency dependence of the real (ε') and imaginary (ε'') parts of the dielectric permittivity at a few representative temperatures above T_m for PSTM-0. Solid lines represent the fitting using equations (2) and (3). A good agreement can be observed between theoretical (solid lines) and experimental values (symbols). Table 3 shows the corresponding adjusting parameters: β, ε_S, ε_∞, and τ. As was described above, the relaxation processes are described by an Arrhenius behavior for the mean relation time, equation (4). Figure 8 shows the Arrhenius behavior corresponding to the mean relaxation time values obtained from the fitting shown in figure 7. The obtained activation energy value of 0.95 eV again shows that the dielectric relaxation processes are closely related to the oxygen vacancies [27], as obtained below T_m.

On the other hand, the frequency–temperature dependence of the dielectric response above T_m for the PSTM-1 and the PSTM-3 samples could not be described by using the

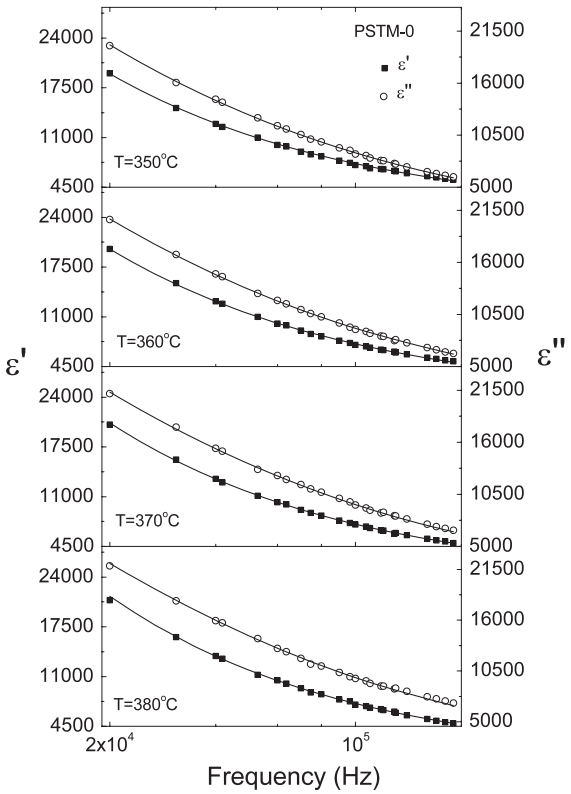

Figure 7. Frequency dependence of the real ε' (■) and imaginary ε'' (○) parts of the dielectric permittivity at a few representative temperatures above T_m for PSTM-0. Solid lines represent the fitting using equations (2) and (3).

Table 3. Adjusting parameters above T_m, obtained from the fitting by using equations (2) and (3).

	PSTM-0			
T (°C)	β	ε_S	ε_∞	τ (s)
350	0.6	172 361	751	0.000 138
360	0.6	166 464	471	0.000 112
370	0.6	142 093	282	0.000 079
380	0.6	133 656	109	0.000 063

semi-empirical complex Cole–Cole equation. Several theories have been proposed to explain the dielectric behavior of different materials after the Cole–Cole model, including the universal relaxation law proposed by Jonscher [30, 43], and a very general model based on the physics of many-body interactions for the interpretation of the dielectric behavior developed by Dissado and Hill [44, 45]. According to Jonscher [30, 43], all solid dielectrics follow fractional power laws in the frequency domain, the interpretations of which depart from the ideal Debye independently relaxing entities. On the other hand, Dissado and Hill [44, 45] have developed a quantum mechanical theory to address the cases that the Debye theory does not solve. In the Dissado–Hill theory [44, 45] for dipolar relaxations, the dipoles are seen as connected with other dipoles through the structure. The theory considers condensed matter as being composed of clusters, with each

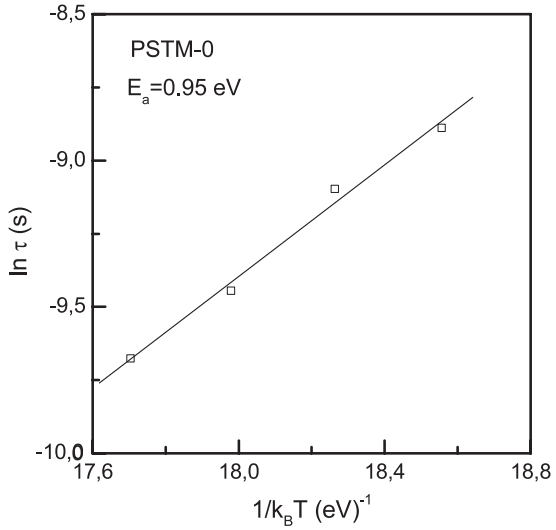

Figure 8. Arrhenius dependence for the relaxation time above T_m for PSTM-0, obtained from the fitting shown in figure 7 by using equations (2) and (3).

Table 4. Fitting power results for the frequency dependence of ε' and ε'' for PSTM-1 and PSTM-3 above T_m.

	PSTM-1		PSTM-3	
	$n-1$		$n-1$	
T (°C)	ε'	ε''	ε'	ε''
350	−0.001	−0.52	−0.004	−0.56
360	−0.001	−0.65	−0.005	−0.60
370	−0.001	−0.72	−0.006	−0.72
380	−0.001	−0.85	−0.007	−0.74

cluster a spatially limited region with a partially regular structural order of individual units. From this assumption, two kinds of interactions are observed, intra-cluster motions and inter-cluster exchanges, and each of these processes will give their own characteristic contribution to the permittivity function.

Figure 9 shows the frequency dependence of the real (ε') and imaginary (ε'') parts of the dielectric permittivity at a few representative temperatures above T_m for PSTM-1 and PSTM-3. The results can be described by a fractional power relation, the universal relaxation law (ε', $\varepsilon'' \propto \omega^{n-1}$) [30]. The solid lines represent the power relation fitting, whose slopes ($n-1$) have been collected in table 4. There is a weak power dependence for the real part of the dielectric permittivity, suggesting near frequency independence, which is characteristic of the behavior of systems with small values of the exponent ($n-1$), in accordance with the known properties of the relevant Kramers–Kronig transforms. However, the imaginary part of the dielectric permittivity shows stronger frequency dependence, which could be associated with conductive processes [30, 43]. The main contribution to the conductive processes could be attributed to space charge in the samples [30, 43] and probably arises from trapped charges in the ceramic/electrode interfaces. It is also observed from

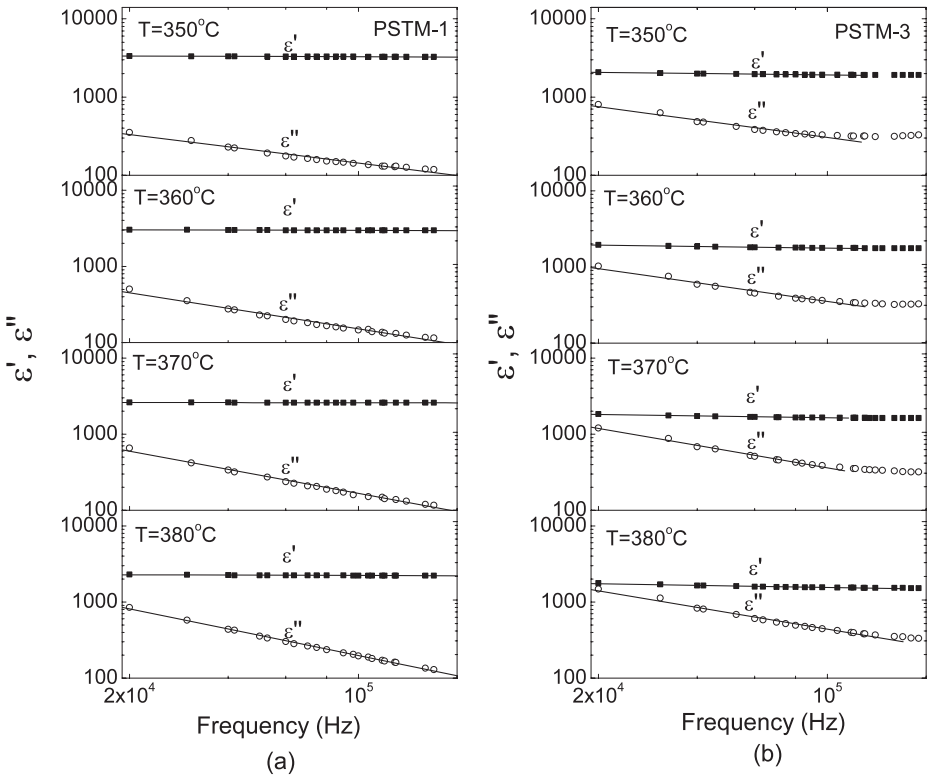

Figure 9. Frequency dependence of the real ε' (■) and imaginary ε'' (○) parts of the dielectric permittivity at a few representative temperatures above T_m for (a) PSTM-1 and (b) PSTM-3. Solid lines represent the fitting using the universal relaxation law. A log–log representation has been used for a better view of the power frequency dependence for the dielectric parameters.

table 4 that the slopes $(n - 1)$ do not change much with manganese concentration in the studied compositions.

The observed behavior for both samples is associated with quasi-dc (QDC) processes, which is usually related to the polarization of slowly mobile ionic and/or electronic charges [30, 43]. Consider the Dissado–Hill theory [44, 45], in the inter-cluster exchange mechanism (QDC relaxation), when an ion hops to an available site over a range larger than the cluster size, its motion is no longer correlated with those of the donor cluster but rather with those of the acceptor cluster. Hence, charge transport over limited distances within the system is regarded as an effective charge displacement from a donor cluster, which becomes ionized, to an acceptor cluster, which becomes charged. As a consequence, an array of clusters exhibiting a distribution of occupying sites will be formed.

Below the transition temperature (T_m), the relaxation process has been associated with oxygen-defect-related dipoles. When the temperature rises the mobility of the oxygen vacancies increases, and above T_m again the relaxation process is related to oxygen vacancies for PSTM-0. For PSTM-1 and PSTM-3, a QDC process could be considered due to the space charges in association with the oxygen vacancies. The hopping conduction of the oxygen vacancies could be considered following an inter-cluster exchange mechanism [44, 45] (QDC relaxation) providing their single and/or double ionization. This hopping process, similar to the reorientation of the dipole, could lead to the dielectric relaxation observed in manganese and samarium modified lead titanate ceramics described by a fractional power relation (universal relaxation law).

Figure 10 shows the frequency dependent conductivity at several temperatures above T_m for the studied samples. Only the UDR term offered a good agreement with the experimental data (solid lines in figure 10) for PSTM-0. For PSTM-1 and PSTM-3, a good fitting was obtained by using both terms of equation (5). The n exponent did not show any temperature dependence [31]. Again, both the dc conductivity and the hopping frequency were found to be thermally activated following the Arrhenius dependence (equations (6) and (7)). Figure 11 shows the Arrhenius dependence for both parameters for the studied samples above T_m, which were obtained from the fitting of the experimental data shown in figure 10. The solid lines represent the fitting using the equations (6) and (7). The activation energy values are shown in the figure.

The ranges of values for U_{dc} are again associated with the ionic conductivity by oxygen vacancies, particularly with doubly ionized [40, 41] oxygen vacancies. Therefore, it is assumed that the electrical conduction is governed by the thermal excitation of carriers from oxygen vacancies. The corresponding U_{dc} values are expected to be lower than those below the ferroelectric–paraelectric phase transition considering that the increase in temperature provides a higher mobility of the charge carriers. However, the PSTM-1 and PSTM-3 samples do not show this behavior. For these samples, considering the increment of oxygen vacancy concentration during sintering [18, 19], it is supposed that the higher concentration of charge carriers provides higher collisions between them, which prevent the dc conductivity. Note that

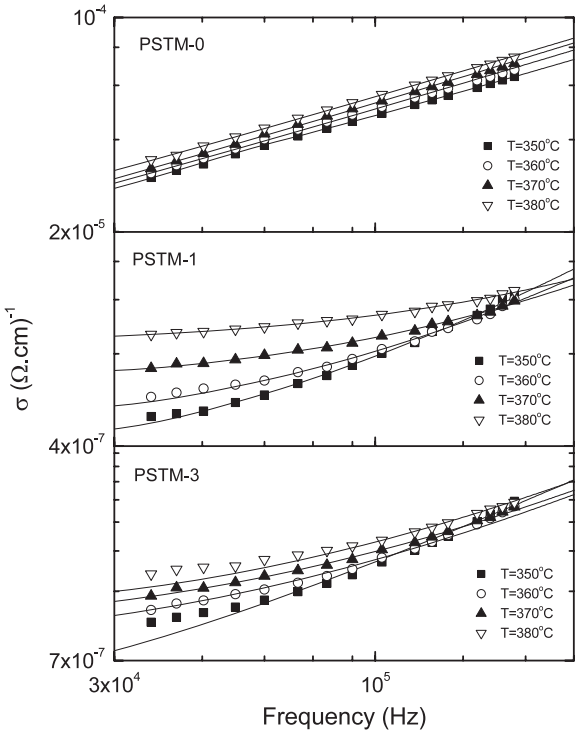

Figure 10. Frequency dependent conductivity data at a few representative temperatures above the ferroelectric–paraelectric phase transition ($T_m = 340\,^{\circ}C$) for PSTM-0, PSTM-1, and PSTM-3. Solid lines represent the fitting using the UDR term of equation (5) for PSTM-0 and both terms (UDR +NCL) for PSTM-1 and PSTM-3.

on increasing the manganese concentration the U_{dc} values increase too, which could be analyzed in the same way.

The activation energy values for the hopping process (U_H) are very far from the U_{dc} values and also from the corresponding values associated with oxygen vacancies. The hopping processes could not be related to the movement of the oxygen vacancies. However, the activation energy values could be associated with relaxations involving thermal motions of titanium ions (Ti^{4+}) [29]. The oxygen vacancies in the PT-based ceramic samples could distort the ionic dipoles due to the Ti^{4+} ions. On the other hand, U_H shows higher values than those below T_m. Above the ferroelectric–paraelectric phase transition, the spontaneous polarization disappears and the hopping processes are prevented by the conductive processes. Also note that the increasing of manganese content prevents the hopping processes too, i.e. the activation energy values increase with the manganese concentration.

4. Conclusions

The dielectric response and the electrical conductivity of the ferroelectric ceramics $(Pb_{0.88}Sm_{0.08})(Ti_{1-x}Mn_x)O_3$, with $x = 0, 1, 3$ at.%, were studied around the ferroelectric–paraelectric phase transition temperature (T_m) in a wide frequency range. The contribution of the manganese doping was evaluated considering the concentration of oxygen vacancies provided by the change of valence in the manganese during sintering. Below the ferroelectric–paraelectric phase transition (T_m), the doubly ionized oxygen vacancies were analyzed as the most likely charge carriers operating in these ceramics and the relaxation processes were associated with the decay of the polarization in the oxygen-defect-related dipoles due to their hopping conduction. In the paraelectric state (above T_m), the electrical conduction was again associated with the doubly ionized oxygen vacancies. However, the hopping processes could not be related to the movement of the oxygen vacancies. The relaxation processes were associated with the distorted ionic dipoles by the oxygen vacancies.

Acknowledgments

The authors wish to thank the Third World Academy of Sciences (RG/PHYS/LA Nos 99-050, 02-225, and 05-043) for financial support and ICTP for financial support of the Latin-American Network of Ferroelectric Materials (NET-43). Thanks to O García-Zaldívar and R de Lahaye.

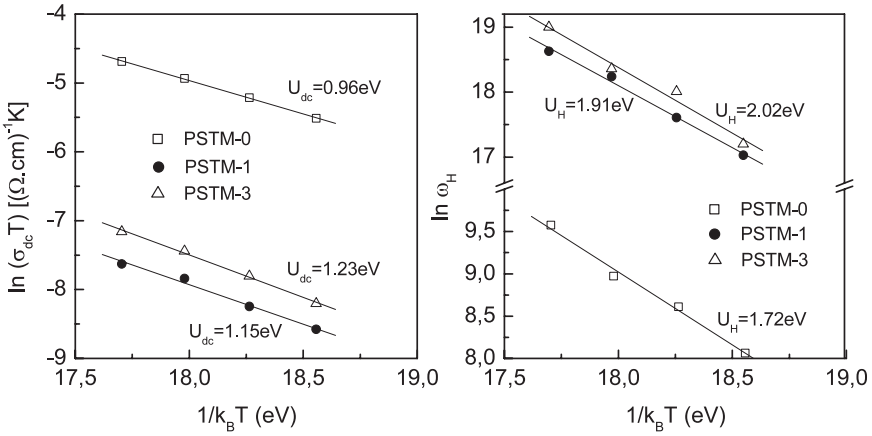

Figure 11. Arrhenius dependence for the dc conductivity (σ_{dc}) and the hopping frequency (ω_H) above T_m for the studied samples. The solid lines are the respective linear fits by using equations (6) and (7).

References

[1] Xu Y 1991 *Ferroelectric Materials and Their Applications* (Amsterdam: Elsevier)
[2] Jaffe B, Cook W and Jaffe H 1971 *Piezoelectric Ceramics* (London: Academic)
[3] Rossetti G A, Cross L E and Cline J P 1995 *J. Mater. Sci.* **30** 24
[4] Hennings D 1971 *Mater. Res. Bull.* **6** 329
[5] Hennings D and Rosenstein G 1971 *Mater. Res. Bull.* **7** 1505
[6] King-Smith R D and Vanderbilt D 1994 *Phys. Rev.* B **49** 5828
[7] Soon H P and Wang J 2006 *J. Appl. Phys.* **100** 124101
[8] Hong C S, Chu S Y, Su W Ch, Chan R Ch, Nien H H and Juang Y D 2007 *J. Appl. Phys.* **101** 054117
[9] Pérez-Martínez O, Calderón F, Pentón A, Suaste E, Rivera M, Leccabue F, Boccelli G and Watts E 1995 *Rev. Mex. Fis.* **41** 85
[10] Pérez Martínez O, Saniger Blesa J M, Peláiz Barranco A and Calderón Piñar F 1999 *J. Mater. Res.* **14** 3083
[11] Das B P, Choudhary R N P and Mahapatra P K 2003 *Mater. Sci. Eng.* B **104** 96
[12] Chen T Y, Chu Sh Y, Wu Sh J and Juang Y D 2003 *Ferroelectrics* **282** 37
[13] Yamashita Y, Yokoyama K, Honda H and Okuma H J 1981 *Appl. Phys.* **20–24** 183
[14] Takeuchi H, Jyomura S, Yamamoto E and Ito Y 1982 *J. Acoust. Soc. Am.* **72** 1114
[15] Duran P, Fdez J F, Capel F and Moure C 1988 *J. Mater. Sci.* **23** 4463
[16] Duran P, Fdez J F, Capel F and Moure C 1989 *J. Mater. Sci.* **24** 447
[17] Ueda I 1972 *Japan. J. Appl. Phys.* **11** 450
[18] Ramírez Rosales D, Zamorano Ulloa R and Pérez Martínez O 2001 *Solid State Commun.* **118** 371
[19] Pérez Martínez O 2001 *PhD Thesis* Physics Faculty, Havana University, Cuba
[20] Cotton F A, Wilkinson G, Wilkinson C A and Bochmann M 1999 *Advanced Inorganic Chemistry* (New York: Wiley)
[21] Takeuchi H, Jhomura S, Nakaya P and Ishikawa Y 1983 *Japan. J. Appl. Phys.* **22** 166
[22] Takeuchi H, Jhomura S and Nakaya P 1985 *Japan. J. Appl. Phys.* **24** 36
[23] Pérez Martínez O, Calderón-Piñar F and Peláiz-Barranco A 2001 *Solid State Commun.* **117** 489
[24] Pérez Martínez O, Saniger J M, Torres-García E, Flores J O, Calderón-Piñar F, Llópiz J C and Peláiz-Barranco A 1997 *J. Mater. Sci. Lett.* **16** 1161
[25] Peláiz-Barranco A, Guerra J D S, Calderón-Piñar F, Aragó C, García-Zaldívar O, López-Noda R, Gonzalo J A and Eiras J A 2008 *J. Mater. Sci.* at press
[26] Cole K S and Cole R H 1941 *J. Chem. Phys.* **9** 341
[27] Poykko S and Chadi D J 2000 *Appl. Phys. Lett.* **76** 499
[28] Steinsvik S, Bugge R, Gjonnes J, Tafto J and Norby T 1997 *J. Phys. Chem. Solids* **58** 969
[29] Maglione M and Belkaoumi M 1992 *Phys. Rev.* B **45** 2029
[30] Jonscher A K 1996 *Universal Relaxation Law* (London: Chelsea Dielectrics)
[31] Nowick A S and Lim B S 2001 *Phys. Rev.* B **63** 184115
[32] León C, Rivera A, Várez A, Sanz J, Santamaría J and Ngai K L 2001 *Phys. Rev. Lett.* **86** 1279
[33] Ngai K L 1993 *Phys. Rev.* B **48** 13481
[34] Funke K 1993 *Prog. Solid State Chem.* **22** 111
[35] Chen A, Yu Z and Cross L E 2000 *Phys. Rev.* B **62** 228
[36] Jiménez B and Vicente J M 1998 *J. Phys. D: Appl. Phys.* **31** 446
[37] Saiful Islam M 2000 *J. Mater. Chem.* **10** 1027
[38] Verdier C, Morrison F D, Lupascu D C and Scott J F 2005 *J. Appl. Phys.* **97** 024107
[39] Yoo H I, Song C R and Lee D K 2002 *J. Electroceram.* **8** 5
[40] Smyth D M 2003 *J. Electroceram.* **11** 89
[41] Bharadwaja S S N and Krupanidhi S B 1999 *J. Appl. Phys.* **86** 5862
[42] Guiffard B, Boucher E, Eyraud L, Lebrun L and Guyomar D 2005 *J. Eur. Ceram. Soc.* **25** 2487
[43] Jonscher A K 1983 *Dielectric Relaxation in Solids* (London: Chelsea Dielectric)
[44] Dissado L A and Hill R M 1983 *Proc. R. Soc. Lond.* **390** 131
[45] Dissado L A and Hill R M 1984 *J. Chem. Soc. Faraday Trans.* **2** 291